Effect of geometry of dipolar orientations on the spectra of dimer and trimer chain aggregates

Kinshuk Banerjee and Gautam Gangopadhyay
S.N. Bose National Centre for Basic Sciences, Block-JD, Sector-III, Salt Lake, Kolkata 700098, India
(Received 30 March 2009; published 7 January 2010)

Here we have considered dimeric and trimeric aggregation of chains where each chain is a conjugated polymer with a definite transition dipole. We have studied the effect of different geometrical orientations of the transition dipoles of the dimer and trimer aggregates on their absorption and luminescence spectra. The excitonic states of the aggregates are symmetry characterized which plays a very important role in deciding the oscillator strength of a particular optical transition. As some realistic applications, we have studied the spectral features of lamellar and herringbone aggregates using dimer model and an explanation is provided for the blueshift in absorption for the cyclic trimer in comparison to its linear counterpart for comparable interchain interactions for thiophene aggregates.

DOI: 10.1103/PhysRevB.81.035307 PACS number(s): 36.20.Kd, 78.20.Bh, 78.66.Qn

I. INTRODUCTION

Small aggregate systems, such as dimer and trimer, are very important because understanding their properties can immensely help to study the physics of large extended samples.[1] It is known for a long time that in composite molecules and aggregates, exciton effects are important[2] and result in the splitting of the excited states with consequent shifts in the spectra. The dimer model, being the simplest, is extensively studied to understand the effect of aggregation on molecular properties.[3–6] This effort has been extended to trimer[7–9] and higher-order aggregates.[10,11] Actually long ago, the spectral behaviors of dimer and trimer systems and their dependence on the orientation of individual monomeric transition dipoles were studied by Kasha *et al.*[12] using only electronic degrees of freedom. Recently Seibt *et al.*[9] studied molecular trimer aggregate spectra including vibrational degrees of freedom.

Luminescence properties of organic π-conjugated polymeric materials are thoroughly studied in the context of light-emitting diodes,[13–15] light-emitting electrochemical cells,[16] photodiodes,[17,18] field-effect transistors,[19–22] and solid-state lasers.[23–25] Interchain aggregate formation in polymer condensed phases has been observed in many polymer materials[26–28] which is essentially responsible for its characteristics emission. For example, in many instances the interchain aggregate formation reduces the luminescence quantum yield and results in redshifted emission.[29–32] Dual luminescence due to the presence of both intrachain and interchain excitons are reported in the photoluminescence studies of poly(*p*-phenylenevinylene) (PPV)-Si nanocomposites[28] and highly regioregular poly(3-hexylthiophene).[26] Spano[33] has shown that for poly(3-hexylthiophene) the entire spectra can be explained by considering only the contribution from interchain aggregate states. His analysis is extended by considering both lamellar (LA) and herringbone (HB) morphologies where it was noted that the 0-0 emission in LA aggregates and the ac-polarized part of the 0-0 emission in HB aggregates get almost quenched but the *b*-polarized component of the 0-0 emission in HB aggregates is present. This was explained with proper orientations of the monomer transition dipoles for LA and HB structures. Recently using a simple nonadiabatic interaction model of dimeric chain aggregation, Bittner *et al.*[6] have explained the dual emission in terms of a strong non-Condon sideband spectra from the lower dipole-forbidden interchain state. In the same line we had generally studied the dimeric chain aggregates[34] to explore the symmetry of the eigenstates and their consequent effect on the absorption and emission spectra and the quantum interference between the vibrational modes due to nonadiabatic interaction. Generalizing the dimeric aggregation of polymer chains we have treated *N*-mer aggregation to show that for equivalent *N*-mers, 0-0 peak is absent in the luminescence spectra.[35] In addition to conjugated polymer aggregate system, trimer aggregates are also important in the studies on vibrational excitons,[36] light-harvesting proteins,[37] and photosynthetic antenna complexes[38] and similar theoretical approach can be followed there.

In this work we have extended our analysis to explore the effect of various geometrical orientations of dipoles of dimer and trimer chain aggregates with both cyclic and linear arrangements and calculated their spectra. We have investigated the characteristics of the excitonic states of the linear and cyclic trimer system to show the dependence of symmetry of the eigenstates due to various orientation of the dipoles. The symmetry of the eigenstates also depend on the interference of vibrational and electronic motion of the interchain species. To get a gross feeling of the combined system comprising of entangled vibrational and electronic motion, we have considered the vibrationless case for the comparison of the complex spectra with the spectra of the pure electronic problem.

In what follows we have discussed on the dressed states of the dimer, cyclic, and linear trimer and treated the problem with vibrational and electronic motion on an equal footing in Sec. II. Section III is devoted for the numerical results and discussion. The paper is concluded in Sec. IV.

II. DRESSED STATES OF THE MODEL N-MER AGGREGATE

We consider the aggregates of *N* number of identical polymer chains where each chain is considered as a mono-

mer containing a single localized exciton[39] and a phonon mode.[6,40,41] The exciton on a particular chain is coupled to all the vibrational modes of the chain aggregate. The Hamiltonian of the aggregate of N number of chains, hereby called as N-mer aggregate, is given by

$$H = \sum_{i=1}^{N} |i\rangle\langle i| \left\{ \epsilon_i + \sum_{k=1}^{N} \left[\hbar\omega_k \left(a_k^\dagger a_k + \frac{1}{2} \right) + \hbar g_{ik} (a_k^\dagger + a_k) \right] \right\} + \sum_{\substack{i,j=1 \\ i \neq j}}^{N} \hbar V_{ij} (|i\rangle\langle j|). \quad (1)$$

Here the exciton on the ith chain is represented as a state vector $|i\rangle$ and ϵ_i is the electronic excitation energy of the ith chain relative to the ground state. $a_k^\dagger, a_k$ are creation and annihilation operators, respectively, for kth vibrational mode with frequency ω_k with g_{ik} being the electron-phonon coupling parameter and V_{ij} being the interchain interaction that transfers the excitation from chain "i" to chain "j." This interaction is taken to be the dipole-dipole interaction given by

$$V_{ij} = \frac{\vec{d}_i \cdot \vec{d}_j}{R_{ij}^3} - 3\frac{(\vec{d}_i \cdot \vec{R}_{ij})(\vec{d}_j \cdot \vec{R}_{ij})}{R_{ij}^5}, \quad (2)$$

where $\vec{d}_i$ is the transition dipole moment of chain i and $\vec{R}_{ij}$ denotes the vector connecting the center of mass of chain i with that of chain j. For identical chains forming the aggregate, the magnitude of all the transition dipoles and $\vec{R}_{ij}$'s are taken to be equal denoted by d and R, respectively. The angle between $\vec{d}_i$ and $\vec{d}_j$ is denoted by θ_{ij}. So for a fixed d and R we can write $V_{ij} = V_{ij}(\theta_{ij})$. Particularly the cases of dimer[6,34] and trimer aggregates, i.e., for $N=2$ and $N=3$, respectively, with various orientations of the transition dipoles are thoroughly discussed.

After applying a standard canonical transformation,[6,42,43] with the unitary operator U, defined as

$$U = \sum_{i=1}^{N} |i\rangle\langle i| \exp\left[-\sum_{k=1}^{N} \frac{g_{ik}}{\omega_k} (a_k^\dagger - a_k) \right], \quad (3)$$

the Hamiltonian in Eq. (1) transforms to the form

$$\tilde{H} = U^\dagger H U = \sum_{i=1}^{N} |i\rangle\langle i| \tilde{\epsilon}_i + \sum_{k=1}^{N} \hbar\omega_k \left(a_k^\dagger a_k + \frac{1}{2} \right) + \sum_{\substack{i,j=1 \\ i \neq j}}^{N} \hbar V_{ij}(\theta_{ij}) |i\rangle \times \langle j| \prod_{m=1}^{N} D_m(\alpha_{ijm}). \quad (4)$$

Here $\tilde{\epsilon}_i$'s are the renormalized energies and $D_m(\alpha_{ijm})$ is the Glauber displacement operator defined as

$$D_m(\alpha_{ijm}) = \exp[\alpha_{ijm}(a_m^\dagger - a_m)], \quad \text{with } i,j,m = 1, \ldots, N,$$

where $\alpha_{ijm} = (\frac{g_{im} - g_{jm}}{\omega_m})$.

The ith eigenstate of the composite system is expressed as

$$|\psi^i\rangle = \sum_{l=1}^{N} \sum_{n_1,\ldots,n_N=0}^{\infty} C^i_{l n_1,\ldots,n_N} |l, n_1, \ldots, n_N\rangle. \quad (5)$$

Here the exciton on the lth chain is defined by the state $|l\rangle$ and $|l, n_1, \ldots, n_N\rangle$ is a direct product state with "n_1" quanta in the first vibrational mode, "n_2" quanta in the second one, and so on. The coefficients "$C^i_{l n_1,\ldots,n_N}$" are complex in general.

Transforming to the coordinate representation, the wave function can be given by

$$|\psi^i(X_1, \ldots, X_N)\rangle = \sum_{l=1}^{N} \sum_{n_1,\ldots,n_N=0}^{\infty} C^i_{l n_1,\ldots,n_N} \prod_{j=1}^{N} \langle X_j | n_j \rangle |l\rangle, \quad (6)$$

where X_j represents the jth phonon coordinate and

$$\langle X_j | n_j \rangle = \left(\frac{\sqrt{\omega_j/\hbar}}{\pi^{1/2} 2^{n_j} n_j!} \right)^{1/2} H_{n_j}(\sqrt{\omega_j/\hbar} X_j) \exp(-\omega_j X_j^2/2\hbar)$$

with H_{n_j} being the Hermite polynomial of order n_j.

In what follows we solve the time-independent Schrödinger equation $\tilde{H}|\psi^i\rangle = \hbar\Omega_i |\psi^i\rangle$ to get the energies Ω_i of the ith eigenstate and the corresponding eigenvectors. Note that the Hamiltonian in Eq. (4) is completely symmetric under the exchange of the indices $(1, \ldots, N)$. Any observable having this property commutes with the corresponding permutation operators.[44] A two-particle-type permutation operator is used in solving the dimer problem and we get the result $C^i_{1 n_1 n_2} = \pm C^i_{2 n_2 n_1}$. Here the (+) sign corresponds to symmetric states and the (−) sign to antisymmetric states.

Now using $N=3$ in Eq. (4), we get the trimer system Hamiltonian and the corresponding wave function is denoted by $|\psi^i\rangle_{trimer}$. At first we consider the interaction among all three monomer chain units and take all the V_{ij} values equal to V to describe a cyclic structure for the trimer. All the angles θ_{ij} are also taken equal to "θ." Applying the two- and three-particle permutation operators on $|\psi^i\rangle_{trimer}$, we finally get the relations between the wave-function coefficients

$$C^i_{1 n_1 n_2 n_3} = \frac{1}{p} C^i_{3 n_2 n_3 n_1}, \quad (7)$$

$$C^i_{2 n_1 n_2 n_3} = \frac{1}{p} C^i_{1 n_2 n_3 n_1}, \quad (8)$$

and

$$C^i_{3 n_1 n_2 n_3} = \frac{1}{p} C^i_{2 n_2 n_3 n_1}, \quad (9)$$

where "p" denotes the set of eigenvalues of the three-particle permutation operator and can assume the three values of the set of cube roots of unity. The detailed derivations are given in the Appendix.

Now for the cyclic trimer system, we get three coupled sets of linear homogeneous equations as in the case of dimer. We take just one of those and using Eqs. (7) and (8), we obtain

$$\sum_{n_1,n_2,n_3} \left\{ \left[\left(n_1+\frac{1}{2}\right)\omega_1 + \left(n_2+\frac{1}{2}\right)\omega_2 + \left(n_3+\frac{1}{2}\right)\omega_3 - \Omega_i \right] \delta_{l_1 n_2}\delta_{l_2 n_3}\delta_{l_3 n_1} + \frac{V(\theta)}{p} D_{1l_1n_1}(\alpha_{121}) D_{2l_2n_2} \times (-\alpha_{122}) D_{3l_3n_3}(\alpha_{123}) + pV(\theta) D_{1l_1n_3}(\alpha_{131}) D_{2l_2n_1}(\alpha_{132}) D_{3l_3n_2}(-\alpha_{133}) \right\} \times C^i_{1n_2n_3n_1} = 0. \quad (10)$$

We solve Eq. (10) to get the eigenvalues and then use the relations Eqs. (7) and (8) to construct the corresponding eigenvectors.

Now to describe the linear arrangement of the trimer system, we take only the nearest-neighbor interactions, i.e., $V_{13}=V_{31}=0.0$. The angles are taken as $\theta_{12}=\theta_{23}=\theta$. The above procedure of using permutation operators and exchange symmetry to find out the eigenstates and their energies is not applicable here. We obtain three coupled sets of linear homogeneous equations for the linear trimer system which are given by

$$\left[\left(l_1+\frac{1}{2}\right)\omega_1 + \left(l_2+\frac{1}{2}\right)\omega_2 + \left(l_3+\frac{1}{2}\right)\omega_3 - \Omega_i \right] C^i_{1l_1l_2l_3} + V_{12}(\theta) \sum_{n_1,n_2,n_3} C^i_{2n_1n_2n_3} \prod_{m=1}^{3} D_{ml_mn_m}(\alpha_{12m}) = 0, \quad (11)$$

$$\left[\left(l_1+\frac{1}{2}\right)\omega_1 + \left(l_2+\frac{1}{2}\right)\omega_2 + \left(l_3+\frac{1}{2}\right)\omega_3 - \Omega_i \right] C^i_{2l_1l_2l_3} + V_{21}(\theta) \sum_{n_1,n_2,n_3} C^i_{1n_1n_2n_3} \prod_{m=1}^{3} D_{ml_mn_m}(\alpha_{21m}) + V_{23}(\theta) \sum_{n_1,n_2,n_3} C^i_{3n_1n_2n_3} \prod_{m=1}^{3} D_{ml_mn_m}(\alpha_{23m}) = 0, \quad (12)$$

and

$$\left[\left(l_1+\frac{1}{2}\right)\omega_1 + \left(l_2+\frac{1}{2}\right)\omega_2 + \left(l_3+\frac{1}{2}\right)\omega_3 - \Omega_i \right] C^i_{3l_1l_2l_3} + V_{32}(\theta) \sum_{n_1,n_2,n_3} C^i_{2n_1n_2n_3} \prod_{m=1}^{3} D_{ml_mn_m}(\alpha_{32m}) = 0. \quad (13)$$

For equivalent chains forming the aggregate, all V_{ij}'s in Eqs. (11)–(13) have the same value $V(\theta)$ and $\alpha_{ijm}=\delta_{im}$ or $-\delta_{jm}$ in all these three equations. Hence comparing Eqs. (11) and (13), we get

$$C^i_{1l_1l_2l_3} = C^i_{3l_1l_2l_3}. \quad (14)$$

Using Eq. (14) in Eq. (12), we have

TABLE I. Energies of the excitonic states (in units of $\hbar\omega_m$) for the dimer, cyclic, and linear trimer systems with their symmetries being indicated in the parentheses. The lowest-energy states (underlined in the table) of all the aggregates studied are antisymmetric with positive interchain coupling, V. The values in the parentheses denote the value of V in each case.

Dimer (V=+0.3)	Cyclic trimer (V=+0.525)	Linear trimer (V=+0.6)
<u>0.849(asym)</u>	<u>1.163(asym)</u>	<u>0.942(asym)</u>
1.062(sym)	1.559(sym)	1.443(sym)
1.850(asym)	2.056(sym)	1.500(asym)
1.895(asym)	2.170(asym)	1.942(asym)
2.064(sym)	2.235(asym)	1.953(asym)
2.122(sym)	2.472(asym)	2.203(sym)

$$C^i_{2l_1l_2l_3} = 2V(\theta) \frac{\sum_{n_1,n_2,n_3} C^i_{1n_1n_2n_3} \prod_{m=1}^{3} D_{ml_mn_m}(\alpha_{21m})}{\left[\Omega_i - \sum_{m=1}^{3} \left(l_m+\frac{1}{2}\right)\omega_m \right]}. \quad (15)$$

Substituting $C^i_{2l_1l_2l_3}$ from Eq. (15) into Eq. (11), we can solve for $C^i_{1l_1l_2l_3}$ and then determine the values of $C^i_{2l_1l_2l_3}$ and $C^i_{3l_1l_2l_3}$ using Eqs. (14) and (15).

III. NUMERICAL RESULTS

In this study we consider all the chains are identical so we take the vibrational frequencies of all the modes to be equal denoted by ω_m. All the parameters and the working equations are scaled with respect to ω_m. The actual value of ω_m is taken as $\hbar\omega_m=0.18$ eV which corresponds to a standard value for C=C stretching frequency in organic conjugated polymers.[6,45]

For two identical chains with parallel transition dipoles, from Eq. (2) we get the interchain interaction as

$$V_{ij} = \frac{d^2}{R^3} \equiv V_0. \quad (16)$$

We take $V_0=0.3$ (in units of ω_m), approximately the value determined by Bittner *et al.*[6] considering transition dipole-dipole interaction between cofacially stacked parallel polymer chains (PPV) and $g_{ik}=\delta_{ik}$.

It is assumed that the vibrational levels of the ground state of an aggregate consisting of N number of polymer chains corresponds to an N-dimensional isotropic harmonic oscillator centered at the origin where $V=0.0$ and $g_{ik}=0.0$ for all i and k. Some energy values (in units of $\hbar\omega_m$) for different aggregate excitonic states are given in Table I. The symmetric and antisymmetric states are indicated with "sym" and "asym," respectively, in the parentheses of the energy values.

For the cyclic trimer system, the antisymmetric states are doubly degenerate. From the energy values of the states of the dimer and trimer systems, we see that the number of states s arising out of splitting due to the nonadiabatic interaction across the zero-phonon levels, can be given by $s=g$

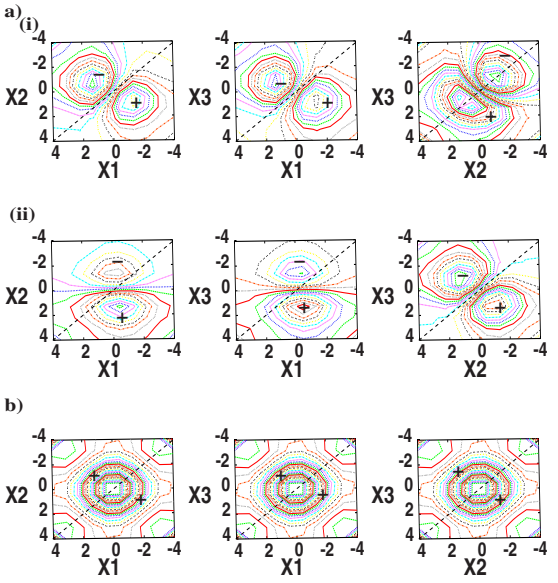

FIG. 1. (Color online) Contour plots of the wave function in coordinate representation of the first two excitonic states of the cyclic trimer system along different phonon coordinate pairs, X_i, X_j $(i,j=1,\ldots,3; i\neq j)$. The dashed line denotes the $X_i=X_j$ line. (a) Antisymmetric state with (i) real and (ii) imaginary parts; (b) symmetric state.

$\times N$; here "g" is the degree of degeneracy of a particular zero-phonon level and "N" is the number of chains. With the positive values of the interchain coupling, V given in Table I, we see that the antisymmetric states are lower in energy than the corresponding symmetric states. This will of course be altered with the change in sign of V.

The contour plots of wave functions in coordinate representation [see Eq. (6)] for the first two excitonic states of the cyclic trimer system are plotted in Fig. 1 against different phonon coordinate pairs, X_i, X_j $(i,j=1,\ldots,3; i\neq j)$. From the plots one can easily identify the symmetric and antisymmetric states. The plots of the antisymmetric state [Fig. 1(a)] show the presence of nodes in both the real and imaginary parts of the wave function. The plots of the symmetric state [Fig. 1(b)] are nodeless and remain unchanged when plotted against any X_i, X_j $(i,j=1,\ldots,3; i\neq j)$ pair, which is not the case with the antisymmetric state. For both types of states though, the overall symmetry across the $X_i=X_j$ line is apparent. The (+) and (−) signs in the contour plots indicate peaks which are above and below the X_i-X_j plane, respectively.

Similar contour plots for the lowest antisymmetric and symmetric excitonic states of the linear trimer system are shown in Fig. 2. It is clear from the plots that the symmetry present across the $X_i=X_j$ line in the case of cyclic trimer system is absent in the linear trimer, as expected. The symmetry present in the case of linear trimer is revealed in Fig. 3; the antisymmetric state shows the presence of nodes and the next state, being nodeless, is symmetric. The reduced symmetry of the linear trimer compared to its cyclic counterpart shows the inherent inequivalency of the linear system although the constituent monomeric chain units are taken to be identical. The inequivalency results from the fact that the nature of the end units in the linear trimer is different from that of the middle one.

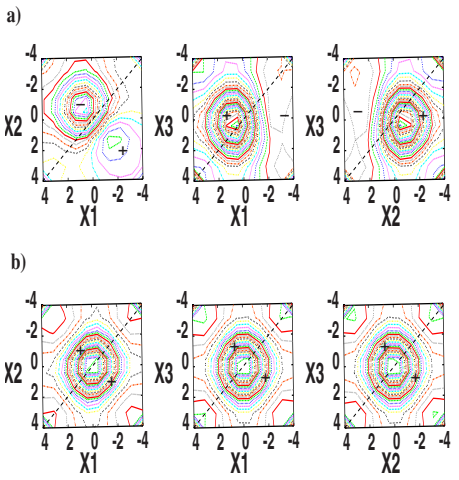

FIG. 2. (Color online) Contour plots of the wave function in coordinate representation of the lowest antisymmetric and symmetric excitonic states of the linear trimer system along different phonon coordinate pairs, X_i, X_j $(i,j=1,\ldots,3; i\neq j)$. The dashed line denotes the $X_i=X_j$ line. (a) Lowest antisymmetric state and (b) lowest symmetric state.

To study the effect of the symmetry classification of the excitonic states of different aggregates and the role played by the orientational geometry of the transition dipoles on the spectra, we have calculated the absorption and emission spectra of different chain-aggregate systems. The emission and absorption spectra are calculated through the Fermi golden-rule expression. We have considered the ground and excitonic states to be in thermal distribution and calculated the spectra at sufficiently low temperature ($T=3$ K) to avoid any kind of thermalized emission and absorption. We also assume a convergence factor γ, which corresponds to very short probing time corresponding to a short pulse laser and the band-shape function is considered as of Lorentzian line shape. We take $\gamma=0.35\omega_m$ for the calculation of spectra.

The transition dipole moment operator of the aggregate $\hat{\mu}_{agg}$, can be written as

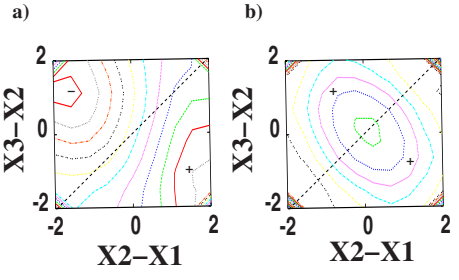

FIG. 3. (Color online) Contour plots of the wave function in coordinate representation of the lowest antisymmetric and symmetric excitonic states of the linear trimer system against relative phonon coordinates, (X_2-X_1) and (X_3-X_2). The dashed line denotes the $X_2=(X_1+X_3)/2$ line. (a) Lowest antisymmetric state and (b) lowest symmetric state.

TABLE II. Transition dipole orientations and the corresponding interchain coupling for the dimer, cyclic, and linear trimer systems.

System	Dipole orientation	Interchain coupling, V
Dimer	Parallel	+0.300
	In line (head to tail)	−0.600
	angular (θ=55°)	+0.102
Cyclic trimer	Triangular (head to tail)	−0.375
	Trigonal (head to head)	+0.525
Linear trimer	In line (head to tail)	−0.600
	In line (head to head)	+0.600
	Angular (θ=45°)	−0.556

$$\hat{\mu}_{agg} = \sum_{i=1}^{N} (\mu_{i,x}\hat{x} + \mu_{i,y}\hat{y})(|i\rangle\langle g| + \text{H.c.}), \tag{17}$$

where $\hat{x}$ and $\hat{y}$ are the unit vectors along X and Y axes, respectively, and $|g\rangle$ denotes the composite ground excitonic state. The magnitude of all the monomeric transition dipoles are taken to be equal as indicated in Sec. II and all the calculated spectra are scaled with respect to it. In Table II, we give the transition dipole orientations considered for the dimer, cyclic, and linear trimer systems and the corresponding interchain interaction, V calculated using Eq. (2).

For all the aggregate systems studied, the dipoles are taken to be on a plane denoted XY plane. The different dipole geometries considered are shown in the diagram of Fig. 4. In the case of the dimer, we consider parallel (θ=0°), in-line (θ=0°), and angular herringbone-type orientations[46,47] (θ=55°) of the transition dipoles. In the angular case, the vector joining the center of mass of the two chains is taken perpendicular to the dipole moment direction. For the two varieties of the trimer system studied, the relative angle between the monomer transition dipole moments, $\vec{d}_i$ are taken like this: the angles between $\vec{d}_1$ and the X axis, between $\vec{d}_2$ and $\vec{d}_1$ and between $\vec{d}_3$ and $\vec{d}_2$ are all taken as equal to θ. For the cyclic trimer system, two structural orientations of the

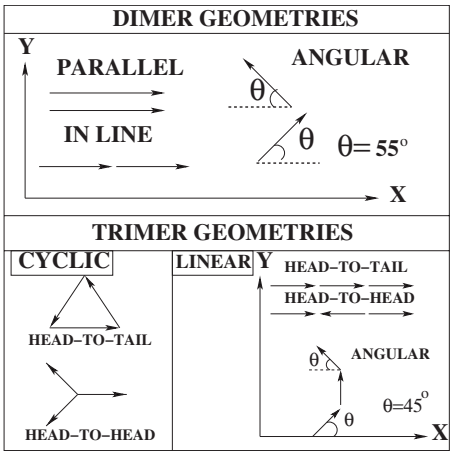

FIG. 4. Schematic of different transition dipole geometries considered for dimer and trimer chain aggregates.

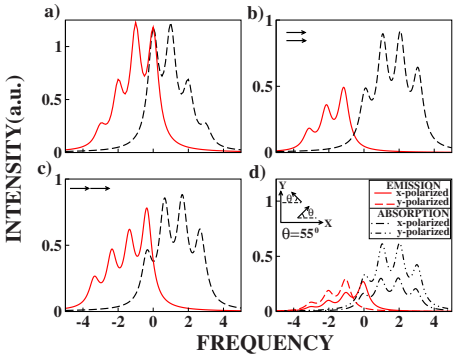

FIG. 5. (Color online) (a)–(c) Emission(solid) and absorption-(dashed) spectra of monomer and dimer with different dipole orientations at T=3 K. (a) the monomer system; (b) dimer with parallel orientation of the monomer dipoles; and (c) dimer with in-line orientation of the monomer dipoles. (d) X- and Y-polarized spectra for the dimer system with the dipoles oriented at 55° in a herringbone fashion at T=3 K.

dipoles are considered. One is the equilateral triangle with the dipoles arranged in a head-to-tail fashion; the other is the trigonal arrangement with all the dipoles meeting at a point. In both the cases the angle is θ=120°. These types of orientations can be physically realized for transition dipoles along the long chain axis and perpendicular to the axis, respectively. The linear trimer system is studied for three distinct dipole orientations; two in-line orientations with head-to-tail and head-to-head arrangements and an angular arrangement with θ=45°.

For the dimer, we plot the emission and absorption spectra for different orientations of the monomeric transition dipoles in Fig. 5 along with the monomer spectra. The monomer shows usual mirror image relation between the emission and the absorption spectra plotted in Fig. 5(a). In case of dimer, for the parallel orientation of the dipoles with positive excitonic coupling V, the oscillator strength is concentrated at the top of the excitonic band.[39] Hence the lowest-energy transition carries very small or zero oscillator strength. This is evident from Fig. 5(b) where there is no 0-0 emission and absorption peak for the dimer for parallel orientation of the dipoles. It corresponds to lamellar aggregate spectra[47] where the 0-0 emission is forbidden. The peak in the absorption spectra, that appears very close to the actual 0-0 peak, is actually due to transition from the ground excitonic state to a higher-lying symmetric excitonic state where the transition energy is very close to the 0-0 transition energy (see Table I). As already mentioned at the start of this section, the vibrational levels of the dimer ground state are taken to be of a two-dimensional isotropic harmonic oscillator where the lowest level is totally symmetric. Since the lowest excitonic state of the dimer is antisymmetric with positive V and there is no thermalized emission, the absence of 0-0 emission peak in this case suggests that optical transition is forbidden from this antisymmetric state to the symmetric lowest ground-state level. Interestingly, for in-line orientation, the 0-0 transition is no more symmetry forbidden and the 0-0 emission peak appears as shown in Fig. 5(c). This is due to the fact that for the in-line head-to-tail arrangement, V is negative (see Table

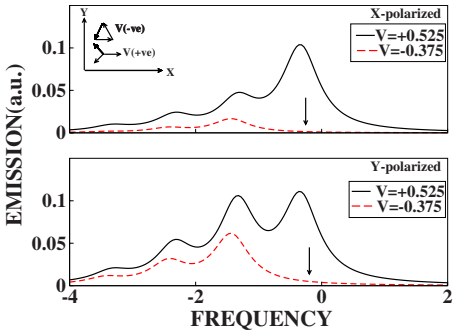

FIG. 6. (Color online) Emission spectra of cyclic trimer system for two different orientations of the monomeric transition dipoles as shown in the upper panel. The angle between the dipoles is 120°. The upper and lower panels contain X- and Y-polarized spectra, respectively. The arrow indicates the position of the 0-0 peak. The spectra are calculated at $T=3$ K.

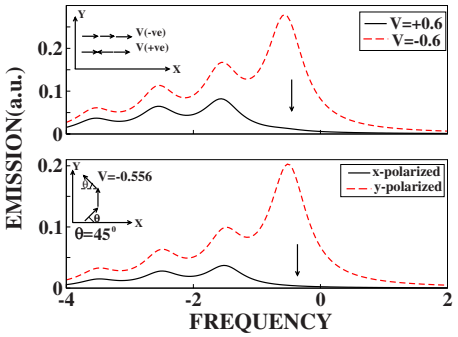

FIG. 7. (Color online) Emission spectra of linear trimer system for three different orientations of the monomeric transition dipoles as shown in the upper and lower panels. The upper panel contains only the X-polarized emission as there is no y component of the dipoles considered. The lower panel contains X- and Y-polarized spectra. The arrow indicates the position of the 0-0 peak. The spectra are calculated at $T=3$ K.

II) and the lowest excitonic state is now symmetric. So the 0-0 transition becomes allowed. The corresponding absorption spectra is apparently not much different from that with parallel dipole orientation [Fig. 5(b)] except it is slightly redshifted due to the fact that the 0-0 peak is truly present here. Its position is very close to the position of the lowest-energy peak (not 0-0) in the absorption spectra of Fig. 5(b), as already mentioned. As there is a manifold of equal number of closely spaced symmetric and antisymmetric excitonic states (see Table I), the sidebands in the absorption spectra show similar nature in both Figs. 5(b) and 5(c) although the relative ordering of energy of these two types of states is opposite in the two cases. The angular orientation ($\theta=55°$) of the dipoles corresponds to herringbone-type arrangement. In the corresponding spectra, plotted in Fig. 5(d), one can see that the 0-0 emission peak is present in the X-polarized emission but is absent in the Y-polarized emission. This result is similar to the experimental results[48–50] obtained from the herringbone oligomer aggregates of p-distyrylbenzene[47] which shows different polarization of the 0-0 emission compared to the sidebands.

For trimer systems, both cyclic and linear, we calculated the polarized emission and absorption spectra for different orientations of the monomer transition dipoles. The X- and Y-polarized emission spectra are shown in Figs. 6 and 7 for cyclic and linear trimer, respectively. From Fig. 6 we observe that for the cyclic trimer, the 0-0 emission is absent for the triangular dipole arrangement with negative coupling V in both X- and Y-polarized spectra. But for the trigonal orientation, the coupling is positive and the 0-0 peak is present in both the X- and Y-polarized emission.

The emission spectra for the linear trimer are shown in Fig. 7. For in-line dipoles, the 0-0 emission peak is present for both positive and negative interchain couplings, V. But for negative V the intensity of the 0-0 peak is very low whereas for positive V the peak is strong (see upper panel of Fig. 7). In the lower panel of Fig. 7 the spectra for angular orientation ($\theta=45°$) is shown. In the X-polarized emission the 0-0 peak is absent but it is present in the corresponding Y-polarized emission. Also the emission spectra of the linear trimer is redshifted compared to that of the cyclic trimer when the interchain couplings are comparable in strength. Similar experimental observations were reported in a study on cyclic and linear thiophene aggregates[51] and was explained using Frenkel exciton theory.

To understand these complex spectral features, specially the presence or absence of the 0-0 emission peak, we have compared the absorption spectra of different aggregate systems with the vibrationless case, i.e., the pure electronic spectra, as shown in Fig. 8. The comparisons are mainly between the electronic absorption peaks and the 0-0 peak in the full vibronic absorption spectra. The electronic spectra are calculated using energy eigenvalues and eigenvectors for dimer and trimer aggregate systems determined from standard expressions for linear and cyclic systems with nearest-neighbor approximation.[39] In case of dimer with parallel and in-line dipole orientations, out of the two possible transitions only one is allowed in each case in the electronic spectra and the two peaks are shifted in opposite directions compared to the position of a monomer peak. In the corresponding full vibronic spectra, the 0-0 absorption for the two dipole orien-

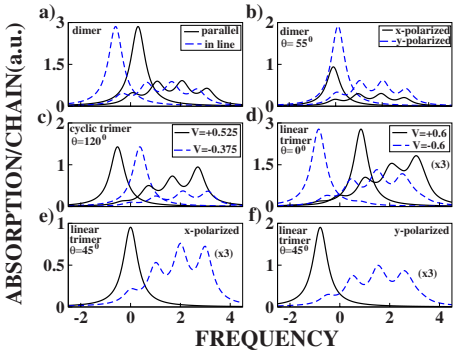

FIG. 8. (Color online) Absorption spectra for different aggregate systems with and without vibrational degrees of freedom considering different orientations of the monomeric transition dipoles. The strong singly peaked spectra correspond to the pure electronic case; the vibronic spectra show the progressions. The angular orientation of the transition dipoles are the same as taken in the previous figures (Figs. 5–7). All the spectra are calculated at $T=3$ K.

TABLE III. Different transition dipole orientations and the corresponding 0-0 emission feature for the dimer, cyclic, and linear trimer systems.

System	Dipole orientation	0-0 emission feature
Dimer	Parallel	Forbidden
	In line (head to tail)	Allowed
	Angular	Allowed in X direction
	(θ=55°)	Forbidden in Y direction
Cyclic trimer	Triangular (head to tail)	Forbidden in both X and Y directions
	Trigonal (head to head)	Allowed in both X and Y directions
Linear trimer	In line (head to tail)	Allowed
	In line (head to head)	Very weakly allowed
	Angular (head to tail)	Forbidden in X direction
	(θ=45°)	Allowed in Y direction

tations show similar behavior, i.e., for parallel dipoles the 0-0 peak is absent but for the in-line case it is present [see Fig. 8(a)]. These shifts are explained similarly on the basis of allowed or forbidden transitions governed by the symmetry of the excitonic states which again depends on the geometry of the transition dipole orientation both for the electronic and the total vibronic case. For angular orientation in the dimer with θ=55°, the presence of 0-0 emission in X-polarized spectra and its absence in the corresponding Y-polarized spectra (see Fig. 5) can also be explained by considering the symmetry of the excitonic states with positive coupling (see Table II) and properly taking the monomer dipole moment components along the two axes. The allowed lowest-energy transition in case of X-polarized spectra and its forbidden nature in the Y-polarized spectra is also evident from Fig. 8(b); the Y-polarized absorption is blueshifted compared to the X-polarized one in both the pure electronic and the total vibronic spectra. Of the two peaks in the electronic spectra of the dimer for angular dipole orientation, one is X polarized and the other is Y polarized [see Fig. 8(b)]. This type of mutually perpendicularly polarized transitions for the dimer in case of angular transition dipoles was also reported in the work of Kasha *et al.*[12] The relative position of the X- and Y-polarized peaks and their intensity also tallies with the 0-0 peak of the full vibronic spectra.

Similar comparisons can be made in the case of both cyclic and linear trimers. We have shown the electronic and vibronic spectra in Figs. 8(c)–8(f) for the same dipole orientations as considered in Figs. 6 and 7 for these systems. The peaks in the electronic spectra and the lowest-energy (0-0) peaks in the full vibronic spectra can be related with similar consideration of symmetry and geometry. For positive interchain interaction, V the antisymmetric electronic state of the cyclic trimer system with energy $-V$ (doubly degenerate) (Ref. 39) is lower in energy and its eigenvector indicates that the transition to a totally symmetric ground state is allowed for the angle θ=120° for both X- and Y-polarized spectra. On the contrary, for negative V the symmetric state with energy $2V$ is the lowest state and the 0-0 transition is forbidden for the angle considered. The full vibronic spectra exhibit the same feature in the context of the 0-0 transition reflected in both emission and absorption spectra. In Fig. 8(c) only X-polarized spectra is shown for all the cases. The Y-polarized spectra is similar and are not shown in the figure.

In the linear trimer, for in-line orientation of the transition dipoles, the lowest-energy transition is weak for positive V and strong for negative V in the electronic absorption spectra shown in Fig. 8(d). So the peak for positive coupling is blueshifted compared to that for negative coupling and the same thing can be noticed in the corresponding full vibronic spectra. These features can be similarly explained with the positioning of the electronic energy levels of the linear trimer for different geometries and the symmetries of the corresponding eigenstates (see Table I). The feature of the lowest-energy transition being weakly allowed for positive V and strongly allowed for negative V is also evident in the emission spectra of the linear trimer with the same geometry (see Fig. 7). For the angular orientation (θ=45°) also, the electronic absorption peak and the 0-0 peak in the full vibronic absorption show similar correspondence in both X- and Y-polarized spectra as is evident from Figs. 8(e) and 8(f). The allowed and forbidden nature of the 0-0 peak in Y- and X-polarized emission, respectively, of the linear trimer system are also explained on the same basis (see Fig. 7). This result also agrees with the study on molecular trimer aggregate spectra,[9] where the forbidden nature of the 0-0 transition was suggested for linear trimer with θ=45°. In Table III we give the nature of the 0-0 emission for various transition dipole orientations of the aggregate systems studied. From Table III it can be noticed that in the context of the appearance of the 0-0 emission peak, the linear trimer is more closely related to the dimer than its cyclic counterpart. This feature is obviously related to the orientation geometries of the monomeric transition dipoles.

IV. CONCLUSION

We have shown the effect of dipolar orientation on the spectral features of the aggregate networks consisting of two or three identical polymer chains. A theoretical methodology is developed to evaluate the dressed eigenstates for dimer, linear, and cyclic trimer aggregates with classification of symmetry of the excitonic states.

It is shown that the 0-0 emission peak in the dimer aggregate may or may not appear depending on the monomeric chain transition dipole orientations. With proper choice of these dipole orientations, we have explained the basic features of LA and HB aggregate spectra. In the case of cyclic trimer, interesting differences are present in the spectra for the transition dipoles along the long chain axis and perpendicular to the axis, specially in the context of the oscillator strength of the 0-0 transition. Similar spectral features are also present in the linear trimer system. In this context, for a gross feeling of the complex vibronic spectra, the pure electronic spectra is calculated for comparison. We have also explained the blueshift in absorption for the cyclic trimer compared to its linear counterpart for comparable interchain interactions for thiophene aggregates[51] which was discussed earlier through Frenkel exciton theory with only electronic degrees of freedom.

The symmetry classification for the excitonic states of dimer and trimer chain aggregates, on the basis of permutation symmetry and wave-function contour plots, can explain the basic spectral features for these systems. The transition dipole geometry plays a crucial role in determining the value of the excitonic energy levels of a particular symmetry that in turn governs the peak intensities. We hope that the quantum statistical properties of the luminescent light can be strongly controlled through the synthetically arranged dipolar orientations of the monomer chains in solid matrix or in a liquid crystal environment.

ACKNOWLEDGMENTS

K.B. acknowledges the Council of Scientific and Industrial Research (CSIR), India for the partial financial support.

APPENDIX: PERMUTATION RELATIONS

The relations among the wave-function coefficients of the cyclic trimer system [Eqs. (7)–(9)] are established using the relevant permutation operators. There are six permutation operators for the trimer system P_{123}, P_{213}, P_{321}, P_{132}, P_{312}, P_{231}. Among these the first one is the identity operator, the next three are *transposition* operators (two-particle-type exchange only), and the last two are three-particle permutation operators.[44] The *transposition* operators are Hermitian as well as unitary with eigenvalue ± 1. Their actions can be shown by taking any one of the six, e.g., $P_{213}|1,n_1,n_2,n_3\rangle=|2,n_2,n_1,n_3\rangle$, where $|1,n_1,n_2,n_3\rangle \equiv |1\rangle|n_1\rangle_1|n_2\rangle_2|n_3\rangle_3$ meaning the oscillator-1 has n_1 quanta, the oscillator-2 has n_2 quanta, and so on. Therefore we obtain

$$\begin{aligned} P_{213}|\psi^j\rangle_{trimer} &= P_{213}\sum_{n_1,n_2,n_3}[C^i_{1n_1n_2n_3}|1,n_1,n_2,n_3\rangle \\ &\quad + C^i_{2n_1n_2n_3}|2,n_1,n_2,n_3\rangle + C^i_{3n_1n_2n_3}|3,n_1,n_2,n_3\rangle)] \\ &= \sum_{n_1,n_2,n_3}[C^i_{1n_1n_2n_3}|2,n_2,n_1,n_3\rangle \\ &\quad + C^i_{2n_1n_2n_3}|1,n_2,n_1,n_3\rangle + C^i_{3n_1n_2n_3}|3,n_2,n_1,n_3\rangle] \\ &= \sum_{n_1,n_2,n_3}[C^i_{1n_2n_1n_3}|2,n_1,n_2,n_3\rangle \\ &\quad + C^i_{2n_2n_1n_3}|1,n_1,n_2,n_3\rangle + C^i_{3n_2n_1n_3}|3,n_1,n_2,n_3\rangle]. \end{aligned} \tag{A1}$$

As $P_{213}|\psi^j\rangle_{trimer}=\pm|\psi^j\rangle_{trimer}$, we get the following exchange relations:

$$C^i_{1n_1n_2n_3}=\pm C^i_{2n_2n_1n_3} \tag{A2}$$

and

$$C^i_{3n_1n_2n_3}=\pm C^i_{3n_2n_1n_3}. \tag{A3}$$

Here the (−) sign in Eq. (A3) is ignored as for an ith normalized eigenstate it gives $C^i_{3n_1n_2n_3}=0$ when all n_1,n_2,n_3 are zero. As $C^i_{30,0,0}=-C^i_{30,0,0}$ implies $C^i_{30,0,0}=0$. Then considering both the plus and minus signs in Eq. (A2), it follows similarly that $C^i_{20,0,0}=0$ and $C^i_{10,0,0}=0$. These results are not meaningful due to the fact that all the wave-function coefficients must be of the same nonzero magnitude for a cyclic structure consisting of identical chains. Hence the minus sign in both the Eqs. (A2) and (A3) is discarded. Then similarly applying the other two *transposition* operators and discarding exchange relations with a negative sign, we get

$$C^i_{1n_1n_2n_3}=C^i_{3n_3n_2n_1} \tag{A4}$$

and

$$C^i_{2n_1n_2n_3}=C^i_{3n_1n_3n_2}. \tag{A5}$$

All these relations are obviously two-particle exchange-type relations. Now from Eq. (A2) (ignoring the minus sign), Eq. (A4), and Eq. (A5), we get the following relations:

$$C^i_{2n_2n_1n_3}=C^i_{3n_3n_2n_1}, \tag{A6}$$

$$C^i_{3n_1n_3n_2}=C^i_{1n_2n_1n_3}, \tag{A7}$$

and

$$C^i_{1n_3n_2n_1}=C^i_{2n_1n_3n_2}. \tag{A8}$$

All these relations are three-particle exchange-type relations derived from the original two-particle exchange-type relations. These exchange relations can also be obtained by considering the action of the three-particle permutation operators on $|\psi^j\rangle_{trimer}$. The eigenvalue of the three-particle permutation operator is denoted by p and can assume the three values from the set of the cube roots of unity, i.e., 1, $\omega(=-\frac{1}{2}+i\frac{\sqrt{3}}{2})$ and $\omega^2(=-\frac{1}{2}-i\frac{\sqrt{3}}{2})$. The above three-particle exchange relations correspond to the real eigenvalue, i.e., $p=1$. To get the exchange relations involving also the complex eigenvalues, we consider the action of a three-particle permutation operator, say P_{231} on $|\psi^j\rangle_{trimer}$. We have

$$P_{231}|\psi^j\rangle_{trimer} = \sum_{n_1,n_2,n_3} [C^i_{1n_1n_2n_3}|2,n_3,n_1,n_2\rangle + C^i_{2n_1n_2n_3}|3,n_3,n_1,n_2\rangle + C^i_{3n_1n_2n_3}|1,n_3,n_1,n_2\rangle] = \sum_{n_1,n_2,n_3} [C^i_{1n_2n_3n_1}|2,n_1,n_2,n_3\rangle + C^i_{2n_2n_3n_1}|3,n_1,n_2,n_3\rangle + C^i_{3n_2n_3n_1}|1,n_1,n_2,n_3\rangle]. \quad \text{(A9)}$$

Now as $P_{231}|\psi^j\rangle_{trimer} = p|\psi^j\rangle_{trimer}$, we get

$$C^i_{1n_1n_2n_3} = \frac{1}{p} C^i_{3n_2n_3n_1}, \quad \text{(A10)}$$

$$C^i_{2n_1n_2n_3} = \frac{1}{p} C^i_{1n_2n_3n_1}, \quad \text{(A11)}$$

and

$$C^i_{3n_1n_2n_3} = \frac{1}{p} C^i_{2n_2n_3n_1}. \quad \text{(A12)}$$

In the Eqs. (A10)–(A12) p can assume any value of the set of cube roots of unity. Operating P_{312} on $|\psi^j\rangle_{trimer}$ will give similar results. For a check, one can notice that Eqs. (A10)–(A12) are identical with the Eqs. (A6)–(A8) for $p=1$.

[1] E. T. Kobayashi, *J-Aggregates* (World Scientific, Singapore, 1996).
[2] A. S. Davydov, *Theory of Molecular Excitons* (McGraw-Hill, New York, 1962).
[3] A. Eisfeld and J. S. Briggs, Chem. Phys. **281**, 61 (2002).
[4] A. Eisfeld and J. S. Briggs, Chem. Phys. **324**, 376 (2006).
[5] J. Seibt, P. Marquetand, V. Engel, Z. Chen, V. Dehm, and F. Würthner, Chem. Phys. **328**, 354 (2006).
[6] E. R. Bittner, S. Karabunarliev, and L. M. Herz, J. Chem. Phys. **126**, 191102 (2007).
[7] H. Eiermann and M. Wagner, J. Chem. Phys. **105**, 6713 (1996).
[8] J. Seibt, V. Dehm, F. Würthner, and V. Engel, J. Chem. Phys. **126**, 164308 (2007).
[9] J. Seibt and V. Engel, Chem. Phys. **347**, 120 (2008).
[10] J. S. Briggs and A. Herzenberg, Mol. Phys. **21**, 865 (1971).
[11] F. C. Spano, J. Chem. Phys. **114**, 5376 (2001).
[12] M. Kasha, H. R. Rawls, and M. A. El-Bayoumi, Pure Appl. Chem. **11**, 371 (1965).
[13] J. H. Burroughes, D. D. C. Bradley, A. R. Brown, R. N. Marks, K. Mackay, R. H. Friend, P. L. Burns, and A. B. Holmes, Nature (London) **347**, 539 (1990).
[14] R. H. Friend, R. W. Gymer, A. B. Holmes, J. H. Burroughes, R. N. Marks, C. Taliani, D. D. C. Bradley, D. A. dos Santos, J. L. Brédas, M. Lögdlund, and W. R. Salaneck, Nature (London) **397**, 121 (1999).
[15] A. J. Heeger, J. Phys. Chem. B **105**, 8475 (2001).
[16] B. Q. Pei, C. Yu, Y. Zhang, Y. Yang, and A. J. Heeger, Science **269**, 1086 (1995).
[17] M. Granstörm, K. Petritsch, A. C. Arias, A. Lux, M. R. Andersson, and R. H. Friend, Nature (London) **395**, 257 (1998).
[18] C. Yu, J. Gao, J. C. Hummelen, F. Wudl, and A. J. Heeger, Science **270**, 1789 (1995).
[19] F. Garnier, G. Horowitz, X. Peng, and D. Fichou, Adv. Mater. (Weinheim, Ger.) **2**, 592 (1990).
[20] Y. Yang and A. J. Heeger, Nature (London) **372**, 344 (1994).
[21] L. Torsi, A. Dodabalapur, L. J. Rothberg, A. W. P. Fung, and H. E. Katz, Science **272**, 1462 (1996).
[22] H. Sirringhaus, N. Tessler, and R. H. Friend, Science **280**, 1741 (1998).
[23] F. Hide, M. A. Diaz-Garcia, B. Schwartz, M. R. Andersson, Q. Pei, and A. J. Heeger, Science **273**, 1833 (1996).
[24] N. Tessler, G. J. Denton, and R. H. Friend, Nature (London) **382**, 695 (1996).
[25] S. V. Frolov, W. Gellermann, M. Ozaki, K. Yoshino, and Z. V. Vardeny, Phys. Rev. Lett. **78**, 729 (1997).
[26] P. J. Brown, D. S. Thomas, A. Köhler, J. S. Wilson, J. S. Kim, C. M. Ramsdale, H. Sirringhaus, and R. H. Friend, Phys. Rev. B **67**, 064203 (2003).
[27] L. M. Herz, C. Silva, R. T. Phillips, S. Setayesh, and K. Müllen, Chem. Phys. Lett. **347**, 318 (2001).
[28] P. K. H. Ho, J. S. Kim, N. Tessler, and R. H. Friend, J. Chem. Phys. **115**, 2709 (2001).
[29] R. Jakubiak, C. J. Collison, W. C. Wan, L. J. Rothberg, and B. R. Hsieh, J. Phys. Chem. A **103**, 2394 (1999).
[30] T. Q. Nguyen, I. B. Martini, J. Liu, and B. J. Schwartz, J. Phys. Chem. B **104**, 237 (2000).
[31] S. Tretiak, A. Saxena, R. L. Martin, and A. R. Bishop, J. Phys. Chem. B **104**, 7029 (2000).
[32] M. Kasha, Radiat. Res. **20**, 55 (1963).
[33] F. C. Spano, J. Chem. Phys. **122**, 234701 (2005).
[34] K. Banerjee and G. Gangopadhyay, J. Chem. Phys. **130**, 084705 (2009).
[35] K. Banerjee and G. Gangopadhyay, J. Phys. B **42**, 165106 (2009).
[36] D. V. Tsivlin, H.-D. Meyer, and V. May, J. Chem. Phys. **124**, 134907 (2006).
[37] J. M. Zhang, Y. J. Shiu, M. Hayashi, K. K. Liang, C. H. Chang, V. Gulbinas, C. M. Yang, T.-S. Yang, H. Z. Wang, Yit-Tsong Chen, and S. H. Lin, J. Phys. Chem. A **105**, 8878 (2001).
[38] R. M. Pearlstein, Photosynth. Res. **31**, 213 (1992).
[39] V. May and O. Kühn, *Charge and Energy Transfer Dynamics in Molecular Systems* (Wiley-VCH, Weinheim, 2004).
[40] R. Friesner and R. Silbey, J. Chem. Phys. **75**, 5630 (1981).
[41] A. Eisfeld, L. Braun, W. T. Strunz, J. S. Briggs, J. Beck, and V. Engel, J. Chem. Phys. **122**, 134103 (2005).
[42] T. Holstein, Ann. Phys. (N.Y.) **8**, 325 (1959).
[43] R. Silbey and R. A. Harris, J. Chem. Phys. **80**, 2615 (1984).
[44] C. Cohen-Tannoudji, B. Diu, and F. Laloë, *Quantum Mechanics* (Wiley-VCH, New York, 2005), Vol. 2.
[45] J. Cornil, D. Beljonne, C. M. Heller, I. H. Campbell, B. K. Laurich, D. L. Smith, D. D. C. Bradley, K. Müllen, and J. L. Brédas, Chem. Phys. Lett. **278**, 139 (1997).

[46] F. C. Spano, J. Chem. Phys. **116**, 5877 (2002).
[47] F. C. Spano, J. Chem. Phys. **118**, 981 (2003).
[48] H.-J. Egelhaaf, J. Gierschner, and D. Oelkrug, Synth. Met. **83**, 221 (1996).
[49] J. Gierschner, H.-J. Egelhaaf, and D. Oelkrug, Synth. Met. **84**, 529 (1997).
[50] D. Oelkrug, A. Tompert, J. Gierschner, H.-J. Egelhaaf, M. Hanach, M. Hohloch, and E. Steinhuber, J. Phys. Chem. B **102**, 1902 (1998).
[51] M. Bednarz, P. Reineker, E. Mena-Osteritz, and P. Bäuerle, J. Lumin. **110**, 225 (2004).